LA-UR

91-256

LA-UR--91-256

DE91 007471

TITLE PULSED POWER CONSIDERATIONS FOR ELECTRON BEAM PUMPED KRYPTON FLUORIDE LASERS FOR INERTIAL CONFINEMENT FUSION APPLICATIONS

AUTHOR(S) E.A.ROSE, T.E.MCDONALD, L.A.ROSOCHA, D.B.HARRIS, J.A.SULLIVAN

Los Alamos National Laboratory

I.D.SMITH

Pulse Sciences, Inc.

SUBMITTED TO SPIE International Symposium on High Power Lasers

24 January 1991, Los Angeles, CA

DISCLAIMER

Los Alamos National Laboratory
Los Alamos, New Mexico 87545

Pulsed-power considerations for electron-beam pumped krypton-fluoride lasers for inertial confinement fusion applications

E.A. Rose, T.E. McDonald, L.A. Rosocha, D.B. Harris, J.A. Sullivan

Los Alamos National Laboratory
Box 1663, Los Alamos, NM 87545

I.D. Smith

Pulse Sciences, Inc.
600 McCormick St, San Leandro, CA 94577

ABSTRACT

The Los Alamos National Laboratory inertial confinement fusion (ICF) program is developing the krypton-fluoride excimer laser for use as an ICF driver. The KrF laser has a number of inherent characteristics that make it a promising driver candidate, such as short wavelength (0.25 μm), broad bandwidth to target (>100 cm^{-1}), pulse-shaping with high dynamic range, and the potential for high overall efficiency (>5%) and repetitive operation. The large KrF laser amplifiers needed for ICF drivers are electron-beam pumped. A key issue for all laser ICF drivers is cost, and a leading cost component of a KrF laser driver is associated with the pulsed power and electron diode. Therefore, the efficient generation of electron beams is a high priority. The Los Alamos ICF program is investigating pulsed-power and diode designs and technologies to further the development of affordable KrF laser ICF drivers.

1. TECHNOLOGY PROGRAM

The pulsed-power system for the laser amplifier is the hardware necessary to transform wall-plug electricity into excimer excitation. It includes the pulsed-power drive circuitry (high voltage generation and pulse shaping) and the electron-beam diode (electron-beam generation and transport to the laser gas).

At Los Alamos, we have endeavored to identify and resolve the electron-beam pumping issues that are critical for scaling KrF amplifiers to the module sizes required for 1) the proposed next-generation laser fusion facility at Los Alamos at 100 kJ and 2) a high-gain facility, the Laboratory Microfusion Facility (LMF), at 3 to 10 MJ.

Major issues include the choice of pulsed-power and electron-diode architectures, the formulation of scaling rules and understanding fundamental physical limitations, development of calculational models for performance prediction and optimization, experimental benchmarking of models, and performance enhancement and cost reduction. Performance enhancement and cost reduction are critical to achieving the goal of constructing practical high-energy ICF systems.

The following are the main elements of emphasis for technology development:

1) pumping system architecture - achieving an efficient match of pulsed-power driver and electron-beam diode and optimizing their connection to the rest of the laser system,

2) diode physics - understanding the basic mechanisms of electron-beam generation, transport, and deposition in the laser gas and optimizing the diode to achieve high efficiency and pumping uniformity (temporal and spatial), and

3) vacuum insulation - determining the physical mechanisms that produce breakdown in the vacuum diode and developing advanced insulator materials to achieve higher operating stresses.

2. SCALING TO HIGHER ENERGY

Los Alamos studies indicate that a reduction in overall system complexity and cost is realized by increasing amplifier sizes. The Los Alamos program plan projects that the LMF system can be reached by a two-stage increase in

amplifier size: from the present 10-kJ Aurora large aperture module (LAM) to a 50-kJ module and ultimately to a 250-kJ module.

2.1 Scaling laws

The impact of increasing amplifier size on the parameters of the pulsed power systems is shown in Table 1.[1] For this exercise, it is assumed that the gas mixture and pressure are held constant, while the dimensions of the laser chamber are varied together (constant aspect ratio) by a factor k. The gain-length product $g_0 L$ is also held constant. The gain g_0, and thus the pump rate P, decrease with increasing amplifier size. The pulse length is increased to maintain a constant specific pump energy (joules per liter). As the amplifier size is increased, the voltage is increased to penetrate and uniformly pump the greater depth of gas. The voltage increase with length is not linear in general; a power of κ is used by way of illustration. The value of κ has far-reaching implications for the pulsed-power parameters. When κ is less than 1 (the standard case), diode impedances decrease and self-magnetic fields increase for increasing amplifier sizes.

To obtain a uniform spatial energy deposition profile, Rosocha[3] scales voltage as $[W \times \rho_{gas}]^{0.6}$ for pure argon, Key[2] and Sullivan as $[W \times (1+\alpha) \times \rho_{gas}]^{0.75}$ for α fractional krypton in argon. Krohn[4] has made detailed Monte-Carlo calculations over the range (V = 0.6 to 1.4 MV, ρ-W product = 0 to 3.3 amagat-meters, α = 0.5). A fit to these data indicate that κ =0.64 is valid for 10% peak-to-average pumping uniformity. (These data can also be fit by the linear function V = 260 kV + 365 $[W \times \rho_{gas}]$ kV.)

Table 1: Scaling relationships for amplifier parameters

Parameter	Original	Scaled
Length, Width, Height	L, W, H	kL, kW, kH
Energy	E	k^3 E
Pump rate	P	P/k
Small-signal gain	g_0	g_0/k
Pulse length	T	kT
Voltage	V	k^{κ} V
Current density	J	$k^{-\kappa}$ J
Total current	I	$k^{2-\kappa}$ I
Impedance	Z	$k^{2\kappa-2}$ Z
E-beam magnetic field	B_{self}	$k^{1-\kappa}$ B_{self}

2.2 Technology development

Increased amplifier size presents challenges to the development of electron-beam pumping technology. The large diode current (J-L product, specifically) requires a large magnetic guide field, which in turn leads to increased diode impedance collapse and electron-beam emission nonuniformities. Large-area diodes present problems with power flow to the emitter, which can lead to nonuniform emission. Diode segmentation may be required to reduce the total current in any one segment and thereby reduce the guide field and power flow problems. However, segmenting the cathode introduces other problems: vacuum voltage holdoff between segments and their current-return structures and regions of unpumped gas between the segments. Thus, two primary development areas are readily apparent: 1) determination of the optimal cathode size and configuration and 2) improvement in the vacuum voltage holdoff of the cathode structure and feedthrough bushing. The improvement of vacuum voltage holdoff has a pervasive beneficial impact on the entire electron-beam pumping system; improvement is not limited to the cathode segmentation issue alone.

A key technology development area is improvement of the electron-beam transport efficiency. Any improvement in this area has high cost-reduction leverage on the entire electron-beam delivery system. Higher beam transport efficiency either a) reduces the required capacity of the pulsed power system and thus reduces its cost or b) provides an amplifier with higher pump power at the same cost. Energy transport efficiencies for large, meter-scale amplifiers are presently on the order of 35% from cathode to gas. At Los Alamos, we believe that the potential exists for achieving efficiencies >60%. Improvements in transport efficiency will likely be achieved through improved materials (foils and hibachi structures) and advanced designs (cathode shaping and emission mapping), rather than by an increase in complexity or investment in additional hardware, which gives this technology area a high cost leverage.

Other electron-beam pumping issues that deserve attention are diode impedance collapse, emission uniformity, energy deposition diagnostics, emitter material lifetime, vacuum-foil lifetime, reflectivity, and chemical compatibility, power-delivery system inductance, energy density of the primary energy storage, and electrical pulselength. However, we do not believe that these issues have the global impact of the three identified above.

3. PULSED POWER

3.1 Pulsed power requirements

The pulsed power requirements are set by the current and voltage needs of the diode to provide the laser pumping power over the duration of laser beam amplification.

Spatial and temporal pumping uniformity requirements are determined by optical damage thresholds and the laser-beam application. Electron-beam spatial inhomogeneities on a small scale tend to be averaged out by the effective integrating action of the laser beam over the length of the laser chamber. Larger inhomogeneities in the beam or, particularly, pumping inhomogeneities that result from nonuniform energy deposition across the laser chamber (electron-beam voltage mismatched to the laser-gas mixture and pressure-width product) will produce spatial nonuniformities in the laser beam. Temporal nonuniformities can arise through voltage variations delivered to the diode or from the impedance collapse of the diode during normal operation.

Standard practice at Los Alamos is to determine a voltage range for diode operation that yields uniform energy deposition in the gas. Then a simulation is performed for the diode with impedance collapse and the pulsed-power system with programmed voltage ramp to determine whether the full system performs to spatial and temporal pumping uniformity specifications.

There are two obvious methods of designing a scaled-up system for a KrF driver:

1) Develop a standard module with set parameters. This module would be efficient and highly reliable. It would be well-developed over the course of several KrF projects and would be improved with experience. Such a building block might be LAM-sized at 10 kJ. A new system would incorporate the number of these modules required to generate the energy.

2) Custom design a new module to fit each system. This is the method employed to date. This method reduces the number of final amplifiers and allows a simplified optical architecture. Module sizes are then defined by the number of liters of excimer gas necessary to extract the energy, the extraction intensity and fluence, and the aperture combination scheme (whereby laser beams are divided, amplified, and recombined).

3.2 Pulsed-power architectures and trade-offs

Three principal options for the pulsed power architecture of KrF laser modules are:

1) the Marx-charged pulse forming line (PFL),
2) the Marx peaking capacitor circuit (PCC), and
3) the Marx pulse forming network (PFN).

The choice from among the architectures is determined mainly by cost, since all have comparable efficiencies. Which is cheapest depends on the pulse duration. The trade-offs are illustrated here for a hypothetical 250-kJ module with a

pump duration of 750 ns that has been studied as a candidate module for the Laboratory Microfusion Facility (LMF). The pulsed-power system must drive a 1-MV, 3.6-MA monolithic diode on each side of the laser.

3.2.1 Marx PFL design

The Marx PFL design is a system of water-filled coaxial or planar transmission lines, which are charged by a Marx bank. The PFLs are discharged into a diode with a matched impedance, producing half the PFL voltage on the diode. These systems are relatively simple to build and operate. For long-pulse durations, however, PFLs become bulky, requiring one meter per 60 ns of diode operating time. Long-pulse operation also involves incurring resistive losses in the water and an additional risk of high-voltage breakdown. PFLs drive the three largest amplifiers in the Los Alamos Aurora laser system.

Solid-dielectric PFLs might be used to good effect, particularly if they could be charged to their operating voltage directly from a power supply, thus eliminating the Marx bank. This architecture would be required to hold off high voltages for long periods. In the absence of a material with a large dielectric constant and high electric stress properties, the system would be long and massive (high propagation speed and low energy storage density). A major disadvantage to solid dielectrics is that they do not recover after high-voltage failures.

Of the three designs, the Marx PFL was studied in most detail for the 250-kJ module because it can be firmly based on existing technology, like the Aurora LAM. The pulsed-power system for one side of the module is illustrated in Figure 1. Uniform drive around the perimeter of a monolithic, nearly square diode is conveniently provided by a hollow square array of twelve coaxial water PFLs. To match the diode, each PFL has an impedance of 3.3 ohms, is charged to 2 MV, and delivers 300 kA at 1 MV. Voltage hold-off requirements determine a PFL diameter of 1.2 meters, and a total pulse duration of 900 ns (including 150-ns risetime) determines a length of 15 meters.

A reasonable charge time for the PFLs is 2.5 μs. A longer charge time would increase both the diameter needed for hold-off and conduction losses in the water. At 2.5 μs, the charging current near peak PFL charge provides ramping of the output pulse to limit the voltage droop to less than 10% as the diode impedance falls (Figure 2). Times shorter than 2.5 μs would introduce pulse distortion. A 2.5-μs charge time for the 1.64-μF capacitance of the PFLs implies a Marx system inductance of $(2.5/\pi)^2 \times 2/1.64 \approx 0.8\,\mu$H. The Marx design uses today's proven, cost-effective, Scyllac-type metal-can capacitors and simple, single-channel spark gaps. This design can readily achieve 0.4 μH per ±100-kV stage, of which twelve are required to reach the open circuit voltage of just over 2 MV. Six Marx banks at 5 μH each are needed in parallel to achieve 0.8 μH.

For this design, the Marx is estimated at 34% of the pulsed-power hardware cost and the PFL and output switches at 66%.

3.2.2 Marx peaking capacitor circuit design

The Marx PCC design is a Marx driving a diode with the aid of a capacitance in parallel with the diode (capacitors or water-filled transmission lines). The peaking capacitor allows the high-inductance Marx to reach near-peak current before being switched into the load, which reduces risetime. This design provides full Marx voltage to the diode. These systems require the design of low-inductance Marx banks. PCCs are used to drive the small aperture module (SAM) in the Aurora system, the Electron-Gun Test Facility (EGTF), and the Laser Scaling Test Bed at Los Alamos.

Figure 3 illustrates the operation of the Marx PCC and compares it to the Marx PFL circuit. The circuit parameters are similar to those of a circuit proposed independently by J.C. Martin. The Marx inductance is too large to drive the diode directly with an acceptable risetime. The peaking switch Sp isolates the diode while the Marx current is established and the peaking capacitance Cp is charged. Cp is chosen so that the peaking capacitor voltage reaches the required diode voltage when the Marx current is near peak and at the minimum of the allowed diode current. When the peaking switch closes, the diode voltage and current rise rapidly to the nominal peak values, followed by a slight fall, since the current flowing out of Cp exceeds the current flowing in. The Marx capacitance is chosen so that the

current then rises back to the nominal value, resulting in the double-humped waveform of Figure 4. The waveform has a 900-ns duration with less than 15% voltage variation.

Unlike the PFL, the PCC does not produce a well-defined end to the pulse, and the pulse must be terminated with diverter switches. These switches would also be present in the PFL circuit for fault protection.

The PCC stores considerably less energy in the peaker (0.35 μF at 1.2 MV = 0.25 MJ) than the PFL (1.64 μF at 2 MV = 3.3 MJ) during a similar effective electric stress time (1.1 - 1.2 μs). The volume of water in the PCC is much less, giving the PCC the advantage of greatly reduced cost. The comparison is detailed below.

In the circuit of Figure 3 the peaker is represented as an ideal capacitor, which implies very low wave impedance and hence a large cross-section, implying high cost. Computer simulations indicate that the wave impedance can be as high as 80% of the diode impedance (0.21 ohms) without introducing excessive ripple into the diode pulse. A Marx PCC was designed using coaxial water lines with the same 1.2-m diameter as the Marx PFL system. The impedance of each line can be reduced from 3.3 to 1.7 ohms because the voltage is halved. Only eight lines (versus twelve) are needed in parallel to give 0.21 ohms, and the lengths are reduced from 15 meters to 2.4 meters.

Another advantage of the PCC over the PFL is that the output switches are smaller and cheaper because they withstand only 1 MV for 0.2 μs instead of 2 MV for 1 μs. Moreover, because they close on a fast-rising part of the waveform, they can probably be self-closing instead of triggered.

The primary disadvantage of the PCC is the lower Marx inductance required - 0.1 μH versus 0.8 μH for the PFL system. This lower inductance could be achieved by using more parallel Marxes, in conjunction with employing careful design, closely spaced ground conductors, and the smaller size of each stage to reduce the inductance from 0.4 μH to 0.25 μH per stage. The total number of Marx stages is then 160 (20 eight-stage Marxes), compared with 72 (6 twelve-stage Marxes) in the PFL system.

Estimates suggest that the Marx PCC cost is 90% (Marx 52%, water lines and switches 38%) of the Marx PFL cost (Marx 34%, water lines and switches 66%), and the PCC has a 20% longer pulse duration. The PCC hardware is half the length of the PFL hardware (11.5 meters from Marx to output switches, versus 23.6 meters), resulting in reduced facility costs. The efficiencies of the two circuits are similar, with the energy diverted on the tail of the PCC pulse roughly equal to that lost in the slow charge of the PFLs.

3.2.3 Marx pulse-forming network

Pulse-Forming Networks (PFNs) are systems of Marx banks in parallel that operate as energy-storage and pulse-shaping circuits. The relatively high inductance of these systems limits their usefulness to longer pulse durations. In addition, pulse shapes can have significant oscillations, unless several harmonics are provided. However, the PFN system experiences the voltage delivered to a matched load for the time of the pulse duration only, leading to a low-stress system. A Los Alamos PFN design for a 2.5-MJ amplifier with a 2-μs pulse duration has been published.[5]

The advances being made in low-inductance, high-energy-density capacitors makes PFNs more attractive for driving lasers at shorter pulse durations. For very large systems, the pulsed power model must deal with both the lumped elements of the PFN capacitor banks and with the distributed parameters of the power distribution system.

Guillemin Type A, C, and E networks have all been used in conjunction with Marx generators to obtain roughly rectangular voltage pulses. For a typical example to compare with the PFL and PCC designs Figure 5 shows a Type C circuit with two sections. The parameter values were chosen to provide a 750-ns pulse into a 0.27-ohm diode with 1 MV average voltage and no more than 15% total voltage variation. The rise-time is about 200 ns. The stored energy (4 MJ) is less than that in the PFL and PCC circuits (5 MJ) because the circuit has no losses associated with water capacitors and energy transfer.

Consider the 1.5-μF, 2.25-MV section. Present technology provides a Marx with twelve $\leq\pm$100-kV stages, 0.4 μH per stage. Assuming a reduction to 0.25 μH per stage, as for the PCC Marx, implies 3 μH total per Marx. Thirty parallel Marxes would be needed to achieve 0.1 μH for the 1.5-μF section. Eighteen more Marxes would be needed to achieve 0.18 μH for the lower capacitance section. There will also be inductance associated with the interconnection of the individual Marx banks and their connection to the diode. Additional parallel Marxes and/or attention to design of the power transmission scheme is indicated. In summary, there are at least 48 Marxes comprising 576 stages in all, and this compares with 72 and 160 stages for the PFL and PCC circuits. Although cost has not been extimated for this PFN design, it is believed to be more expensive than the PFL and PCC systems.

The required inductance for the PFN elements increases as the square of the pulse duration. Thus, for a 1.5-μs pulse of the same voltage and energy, the number of parallel Marxes in the above example is reduced to twelve (48/4), and the PFN has fewer total stages than the PCC circuit. Because no water lines are needed, the Marx PFN should be the cheapest approach in this time range.

Improvements in Marx technology may make the PFN cost-competitive with the PCC or PFL, even at pulse lengths below 1 μs. One recent development has been higher energy-density capacitors. By themselves these are of limited benefit. Increasing the energy density in a given Marx configuration actually increases the time required to extract the energy by increasing capacitance. Decreasing the capacitor size at fixed capacitance helps, but only weakly, because most inductance is in the spark gaps. What is needed is a cheap, high energy-density Marx with low inductance. Compared with the metal-can examples described above, which have about 2 μH/MV, plastic-cased capacitor Marxes,[6] have achieved 0.6 μH/MV. Multichannel switches have allowed less than 0.2 μH/MV,[7] but this has only been demonstrated in two-stage Marxes. These decreases in inductance could lead to cheaper PCC or PFN modules at less than 1 μs, provided the cost per joule of the Marx can be kept comparable to that of present Marxes.

3.2.4 Summary of trade-offs

Present 0.5-μs KrF laser modules use Marx pulse forming lines. For pulse durations in the 0.75 to 1 μs range, Marx peaking circuits may be cheaper and more compact, and in the 1 to 1.5 μs range Marx PFNs may be preferred. The development of low-inductance, high-energy Marxes, perhaps with high energy-density capacitors, may extend the advantages of the PFN and PCC to shorter pulse durations if they can be achieved with little or no increase in cost per joule.

4. DIODE

4.1 Diode foils

The diode foil is required to separate the vacuum of the diode from the laser gas. It must be highly transmissive to the electrons (thin and low-Z), strong enough to support the gas pressure over the extent of the hibachi openings during pumping to withstand heating and gas pressure jump, chemically inert to the fluorine of the laser gas, and low-reflectivity in the UV to suppress amplified spontaneous emission (ASE) and parasitics. The damage threshold of the diode foil is a basic limitation on the pumping of an amplifier.

Each area element dA of the diode pair is required to deliver energy to a mass $dA \times W \times \rho_{gas}$, at specific pump energy dE (energy per unit mass). The energy stopped per unit area of the foil can be expressed as $F/[1-F] \times dE \times W \times \rho_{gas}$, where F is the voltage- and thickness-dependent fractional loss of energy to the foil. Note that F also depends on the details of the backscattering of electrons from the laser gas and the transmission of electrons through the gas from the opposing diode. Energy losses calculated from tabular data (dE/dx tables) have been compared with results from the Los Alamos Monte Carlo code DEP3D, which includes backscattering and transmission effects. For the LAM, the tabular data gave foil losses which were less than half the DEP3D losses.

One can argue that the ratio of the specific energies delivered to the foil and the gas remains constant as voltage is scaled upward, since the ratio of energy-loss coefficients $dE/dx_{gas} \div dE/dx_{foil}$ remains reasonably constant. This argument should hold for the foil and the gas adjacent to it, since they are subjected to similar electron environments.

The situation is complicated, however, because energy deposition is not in the range-thin regime and because a pumping uniformity criterion is applied to determine the operating voltage.

Preliminary analysis of the DEP3D calculations (V = 0.6 to 1.4 MV, 10% peak-to-average pumping uniformity, 50% krypton, 51-μm titanium diode foils) indicates that foil losses decrease slightly (about 15%) with increasing voltage over this range. The decrease in the factor F/[1-F] outweighs the increase in the factor $W \times \rho_{gas}$ with increasing voltage. This trend is encouraging for scaling to larger amplifiers.

4.2 Diode electrical stress

A materials-related limitation on diode pumping has been proposed by McGeoch.[8] In this scenario, bombardment of the anode releases gases which lead to electrical breakdown in the diode. A scaling exercise performed by Rosocha[3] indicates that the maximal specific pump energy is reduced for wider amplifiers. This conclusion has some negative implications for scaling to larger amplifier sizes.

4.3 Diode operation

The Los Alamos program has employed cold-cathode, field-emission diodes with carbon felt or velvet emitters. The impedance of the diodes is time-dependent because the diode impedance falls with time (impedance collapse). This phenomenon is apparently due to the expansion of the electron-emitting plasma on the surface of the cathode. It has been observed at Los Alamos and elsewhere that higher magnetic fields increase the rate of diode closure and also induce the formation of hot spots (regions of significantly higher current density). High rates of diode closure reduce the time during which the diode can be operated, and hot spots increase the heat loading on the foil.

4.4 Diode architectures

A guide magnetic field must be applied to large-area, high-current diodes to prevent electron-beam pinching from self-magnetic forces. Experience at Aurora has shown that an external field equal to 1.5 times the maximal self field is sufficient. As monolithic diode sizes grow with larger scale amplifier modules, the magnetic field strength required also grows. The cost of magnetic field coils and hardware grows rapidly, in some scenarios outstripping the power delivery capabilities of the site and requiring cryogenic coils or inertial energy storage capability.

High applied magnetic fields increase the rate of impedance collapse, which limits the time that the diode can be operated.

One solution to the problem is to subdivide the diode into segments separated by a return-current path. This isolates the self-magnetic fields of the segments from each other and reduces the magnetic field requirements. The pulsed-power driver elements are also isolated from each other. However, diode segmentation introduces unpumped regions in the gas between segments. These dead spaces add absorption losses. Vertically oriented segments cause the laser beam to encounter pumped and unpumped regions in succession. Horizontally oriented segmentation is equivalent to splitting the laser into individual stacked lasers. In the vertically oriented scheme, the diode current density is increased to offset the reduced area of emission, rather than increasing the laser length. To reduce the extent of unpumped gas, diode segments are positioned as closely as possible, which pushes the vacuum electric stress limits.

5. AURORA - THE LOS ALAMOS KJ-CLASS ICF LASER SYSTEM

The Aurora facility[9,10] at Los Alamos is the first large-scale KrF laser fusion system. It employs optical angular multiplexing and serial amplification to deliver kJ-level laser pulses of 5-ns duration to ICF targets.

Figure 6 shows a conceptual layout of Aurora. This system is presently configured to deliver 48 of 96 beams into a single pulse on target. To date, 1.3 kJ in 36 beams (twelve blocked for diagnostics) at 220 TW/cm2 has been obtained in the target chamber.[11] Table 2 summarizes the performance of the Aurora system.

Table 2: Aurora performance

Parameter	SAM	PA	IA	LAM
Pump rate (kW/cc)	215	115	42	125
Small-signal gain (%/cm)	3.0	2.2	1.0	2.3
Laser energy in (joule)	0.2	0.3	40	250
Laser energy out (joule)	3.0	50	300	4500
Stage gain	15	165	7.5	18

5.1 Amplifiers

In order of increasing size, the four laser amplifiers at Aurora are the Small Aperture Module (SAM), Preamplifier (PA), Intermediate Amplifier (IA), and Large Aperture Module (LAM). Current amplifier parameters are summarized in Table 3. (These parameters were not the ones in effect during the 1.3-kJ target shot.) The LAM was constructed early in the project to demonstrate the scalability of electron-beam-pumped amplifiers to large volumes. Its output was 10.7 kJ in 650 ns when operated as an unstable resonator.

Table 3: Aurora amplifiers

Parameter	SAM	PA	IA	LAM
Emitter area (cm^2)	100 x 12	290 x 20	295 x 40	212 x 100
Diode voltage (kV)	320	520	520	650
Pulse length (ns)	200	650	650	650
Diode impedance (ohm)	8	2.7	2.7	1.5
Anode-cathode gap (cm)	3.2	5.8	8	8
Current density (A/cm^2)	30	40	20	25
Hibachi openings (cm)	7.0 x 13.7	7.5 x 22.6	5.8 x 11.3	3.6 x 23.8
Laser aperture (cm^2)	10 x 12	20 x 20	40 x 40	100 x 100

5.2 Marx generators and pulse-forming lines

The three largest amplifiers are powered by Marx PFLs and the SAM by a Marx PCC. The LAM uses double-sided pumping with two PFL's per diode, and the PA and IA use single-sided pumping with a single PFL. The PA, IA, and LAM employ 15-stage Marxes[12] with an open-circuit voltage of 1.8 MV (1.6 MV when charging the PFLs). The PFLs are coaxial lines filled with deionized water. Their dimensions are: 61 cm inner diameter, 91 cm outer diameter, 10.8 m length, 3 ohm impedance, 325 ns one-way transit time, and 100-150 kJ per line. Each PFL is connected to the diode through a trigatron switch and a vacuum-feed bushing, both filled with SF_6. Ouput switches are triggered from 1.6 to 2.1 μs after Marx erection, and a pulse of one-half the charge voltage and twice the PFL transit time is delivered to the cathode. Figure 8 shows an equivalent electrical circuit for one side of the LAM.

5.3 Diode assemblies

The diodes consist of bushing, cathode corona shell, emitter, anode, hibachi, and foil in a vacuum enclosure maintained at 5 μtorr. The diode bushing makes the electrical connection from the output switch to the cathode. This bushing uses 45-degree acrylic insulator rings alternating with aluminum field-grading rings. The cathode corona shell is connected to the bushing, and graphite felt is attached to a contoured boss on the shell to form the emitter. Graphite felt exhibits a low ignition voltage and reasonably uniform electron emission, making it a good choice for these field-emission diodes.

The electrons must pass through a 50-μm titanium foil and an aluminum support structure (hibachi) to reach the laser gas. The high current-density SAM and PA also have 12-μm titanium prefoils to protect the pressure-bearing foils from hot spots. The hibachis have nominal geometrical transmissions of 80-90%. They are designed to support pressure differentials of 600 to 1200 torr. Magnetic guide fields of 1 to 2 kG are employed to enhance the transport efficiency, but it is less than 50%.

Figure 7 shows a cross section of the LAM diode.

A program is in progress to increase the electron transport efficiency of the diodes. Electron trajectories are being modeled for particular diode geometries and conditions. Hibachis are being redesigned to be more transmissive. The size of the hibachi openings was increased on the SAM and PA, and better transport has been observed. An effort is also underway to develop new composite foil materials of high tensile strength and high electron transmission to extend the range of hibachi openings which can be spanned.

6. SUMMARY

Meeting the cost and performance goals of future KrF lasers systems requires significant extensions of existing pulsed-power, electron-diode, and vacuum-insulation technology. To achieve these technology extensions we have identified key cost and performance leverage areas, implemented development programs, and made progress toward optimizing the electron-beam pumping system for megajoule-class KrF lasers.

7. REFERENCES

1. L. A. Rosocha, S. J. Czuchlewski, B. J. Krohn, and J. McLeod, "Excimer lasers for inertial confinement fusion," Los Alamos National Laboratory, LA-UR-90-169, 1990.

2. M. H. Key, M. J. Shaw, I. N. Ross, P. A. Rodgers, and M. C. Gower, "Analysis of high power KrF laser systems," Rutherford Appleton Laboratory, RAL-89-133, 1989.

3. L. A. Rosocha, G. R. Allen, R. G. Anderson, E. M. Honig, M. E. Jones, M. Kang, C. R. Mansfield, H. Oona, E. A. Rose, R. P. Shurter, and V. A. Thomas, "An overview of progress in electron beam pumping technology for KrF lasers," Second Workshop on KrF Laser Technology, Sept 1990, Banff, Canada.

4. B. J. Krohn, H. H. Hsu, and J. C. Comly, "Calculated uniformity and efficiency of e-beam energy deposition in large KrF laser cavities," Los Alamos National Laboratory, T-12(90)BK02, 1990.

5. E. A. Rose, D. E. Hanson, M. Kang, B. J. Krohn, and J. McLeod, "A megajoule class krypton fluoride amplifier for single shot, high gain ICF application," Fusion Technology, 15, 364, 1989.

6. I. D. Smith, and H. Aslin, "Pulsed power for EMP simulators," IEEE Transactions on Antennas and Propagation, AP-26, 1, January 1978.

7. I. D. Smith, et al, "Measurements of a low-impedance large-area 100-kV diode," International Conference on Energy Storage and Switching, November 1974.

8. M. W. McGeoch, "Scaling issues in electron beam diodes," Los Alamos National Laboratory Workshop on Large Area Electron Beam Diodes, Monterey, CA, June 1989.

9. L. A. Rosocha and K. B. Riepe, "Electron-Beam Sources for Pumping Large Aperture KrF Laser," Fusion Technology, 11, 576 (1987).

10. L. A. Rosocha, J. A. Hanlon, J. McLeod, M. Kang, B. L. Kortegaard, M. D. Burrows, and P. S. Bowling, "Aurora Multikilojoule KrF Laser System Prototype for Inertial Confinement Fusion," Fusion Technology, 11, 497 (1987).

11. J.E. Jones, S.J. Czuchlewski, T.P. Turner, R.G. Watt, S.J. Thomas, D.A. Netz, C.R. Tallman, J.M. Mack, and J.F. Figueira, "Performance of the Aurora KrF ICF Laser System," International Conference on Lasers '89, New Orleans, LA, December, 1989.

12. K.B. Riepe, L.L. Barrone, K.J. Bickford, and G.H. Livermore, "Antares Prototype 300-kJ 250-kA Marx Generator," Los Alamos National Laboratory Report, LA-8491, January, 1981.

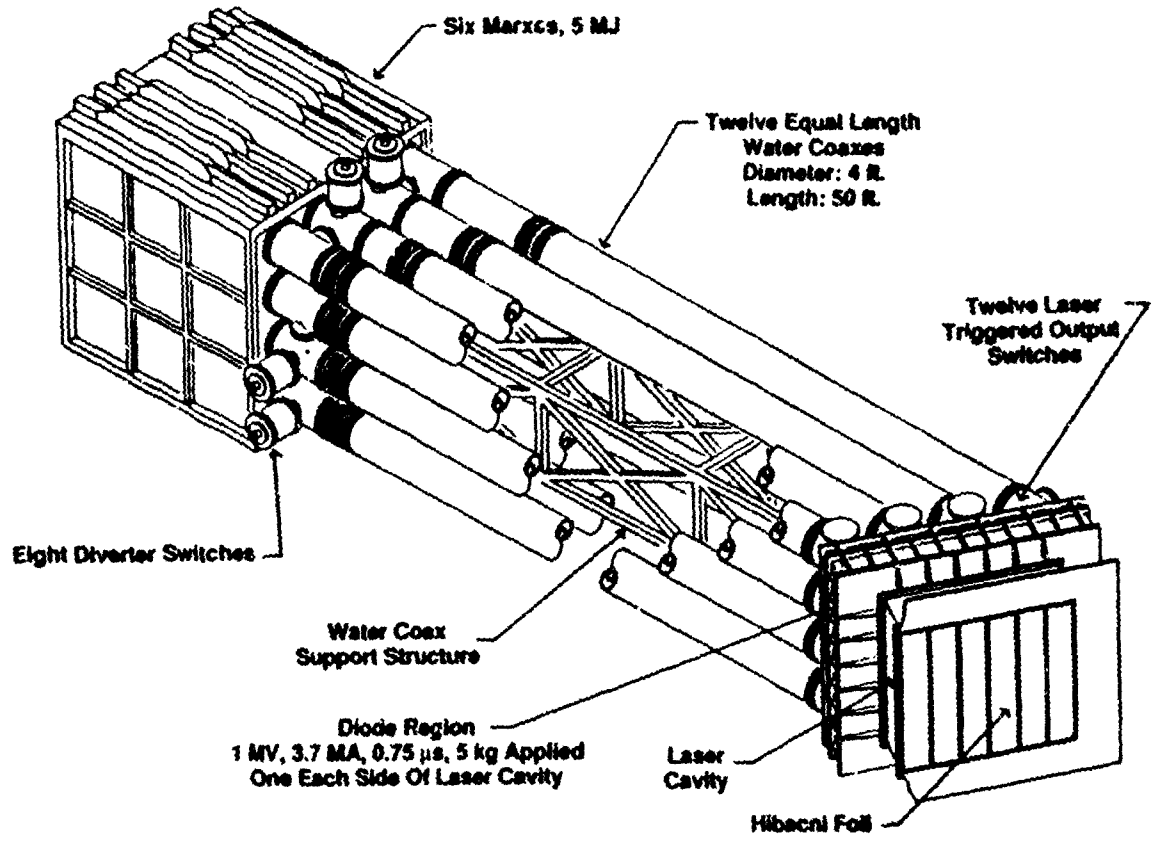

Figure 1: Marx-charged pulse forming line design for a 250-kJ module.

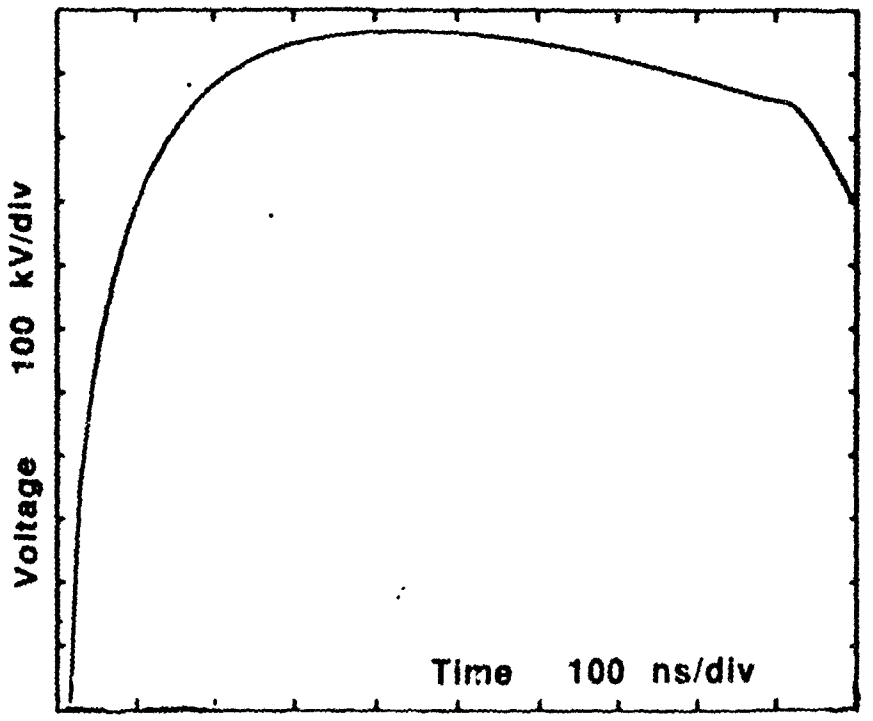

Figure 2: Diode voltage for Marx PFL design, with compensation for diode impedance collapse.

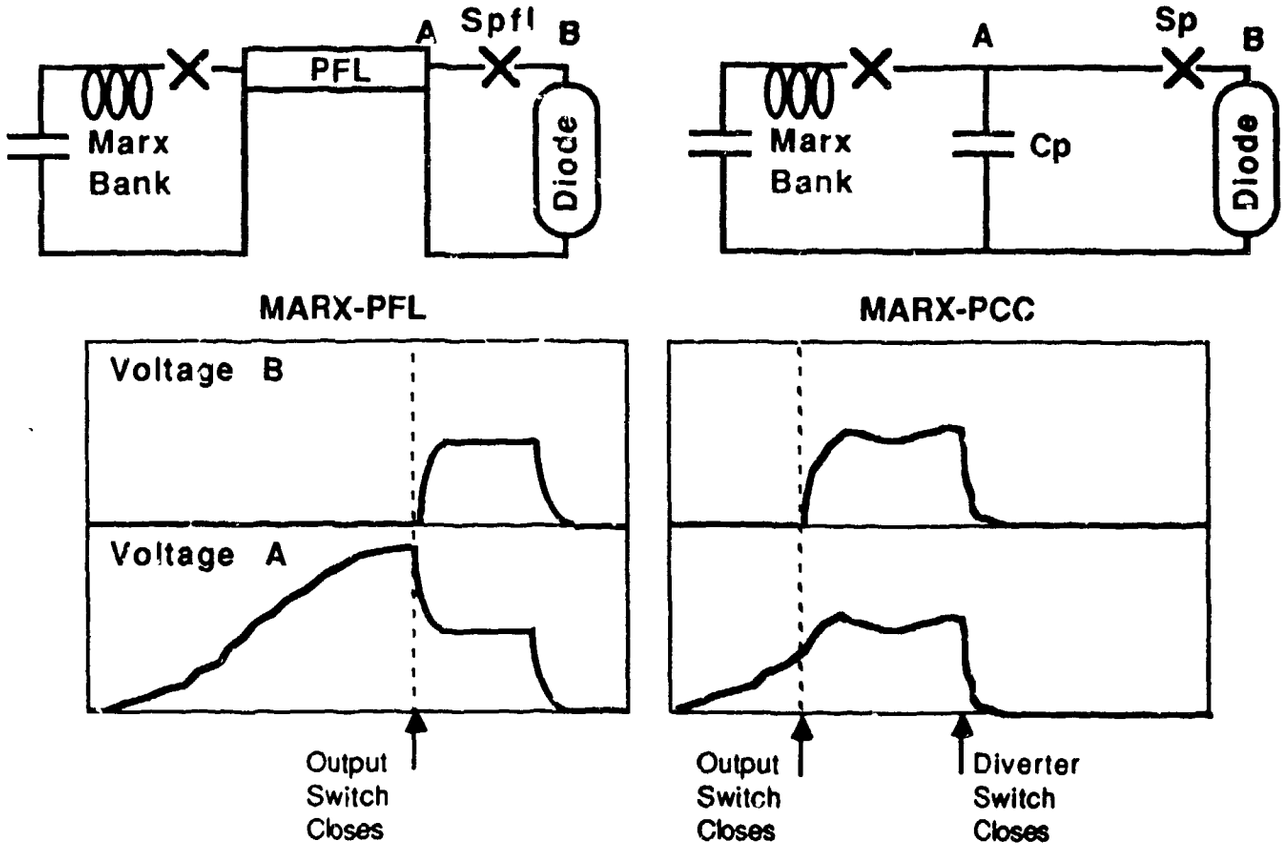

Figure 3: Comparison of the Marx-charged pulse forming line circuit (left) and the Marx peaking capacitor circuit (right). Voltages are shown at the output of the PFL and Cp (Voltage A) and as applied to the diode (Voltage B).

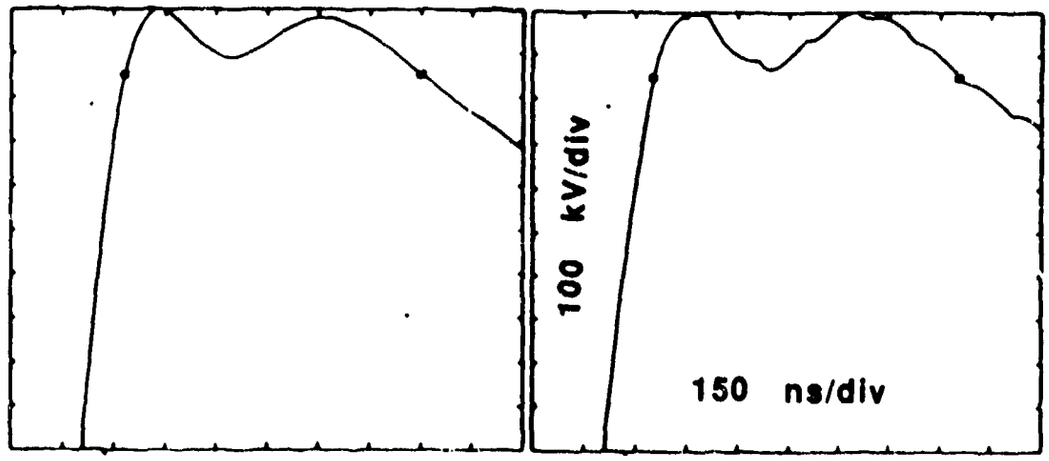

Figure 4: Diode voltage waveforms for Marx peaking capacitor circuit with ideal capacitor (left) and distributed capacitance (right). The distributed capicitance consists of eight 1.7-ohm water lines of length 2.4 meters in parallel.

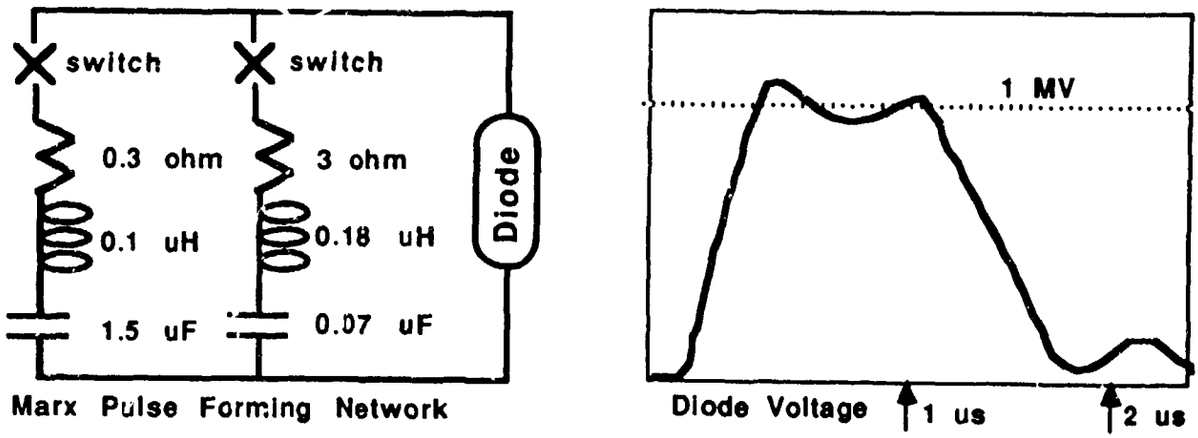

Figure 5: Marx pulse forming network circuit diagram and voltage waveform applied to diode.

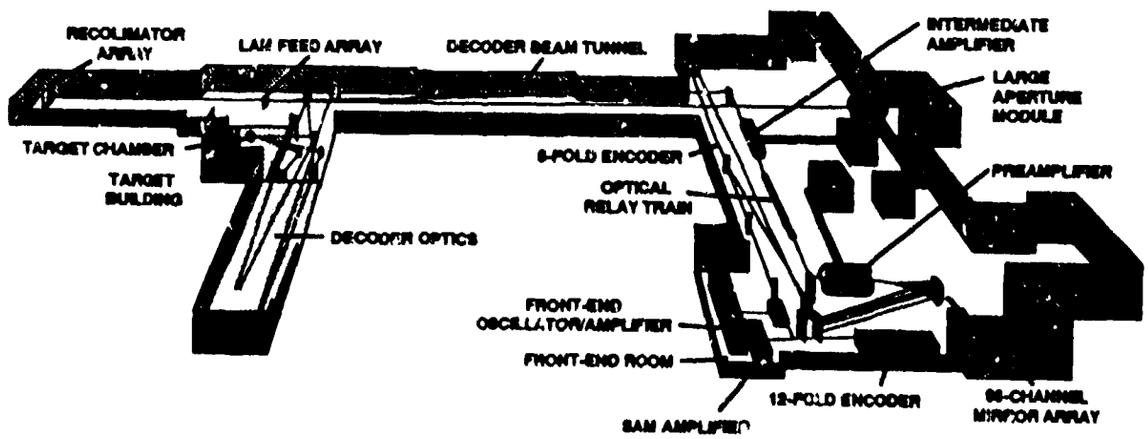

Figure 6: Los Alamos Aurora KrF laser system layout.

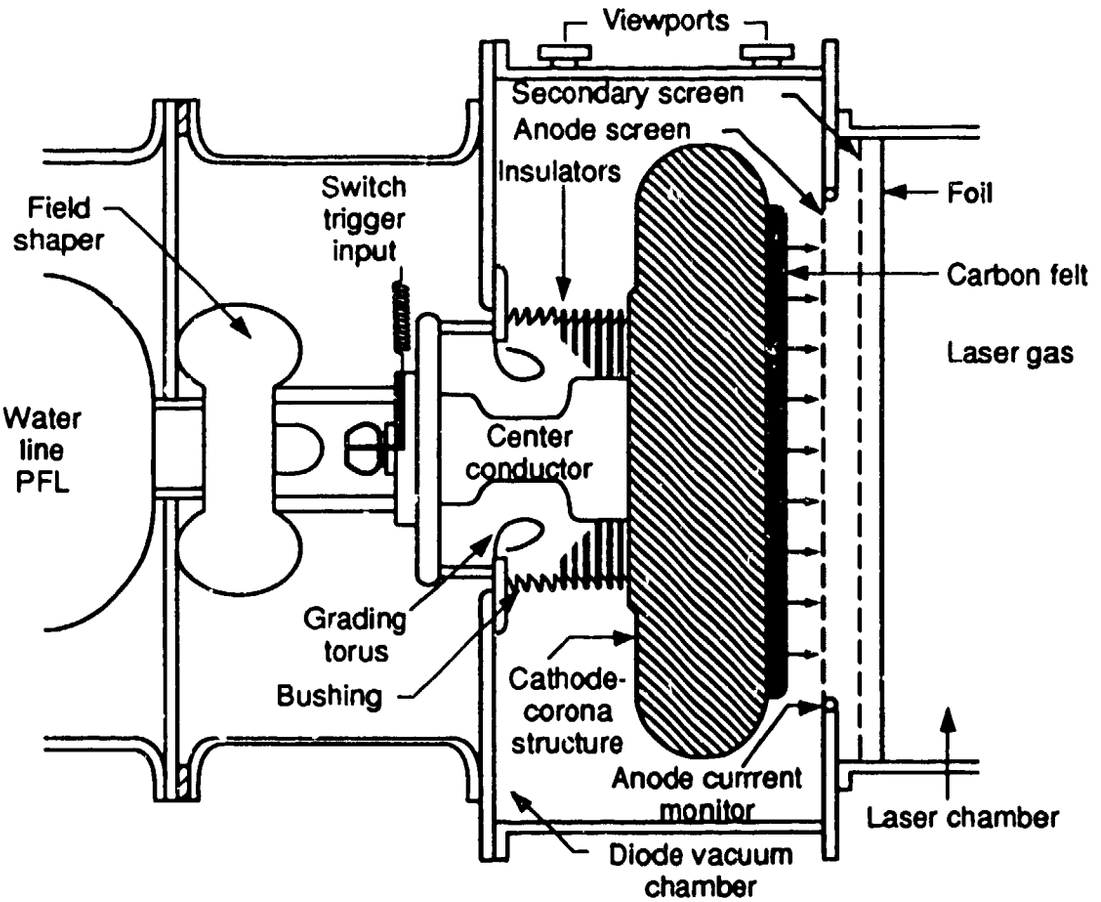

Figure 7: Large Aperture Module (LAM) diode is representative of Aurora diode architectures.

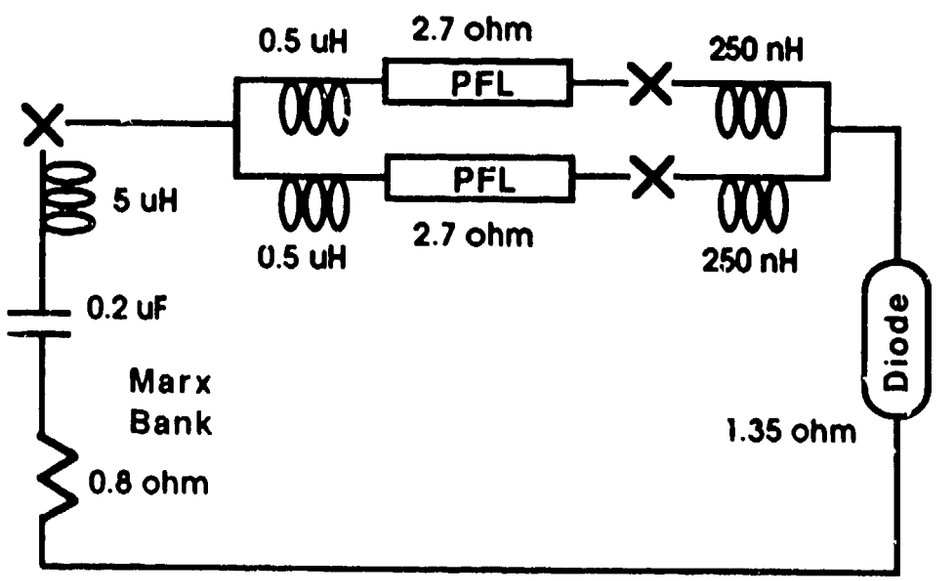

Figure 8: Simplified LAM lumped parameter equivalent electrical circuit.